LEEIXS and XPS studies of reactive unbalanced magnetron sputtered chromium oxynitride thin films with air

Agouram, Said; Bodart, Franz; Terwagne, Guy

Published in:
Journal of Electron Spectroscopy and Related Phenomena

Publication date:
2004

Document Version
Peer reviewed version

Available online at www.sciencedirect.com
SCIENCE DIRECT®
ELSEVIER
Journal of Electron Spectroscopy and Related Phenomena 134 (2004) 173–181
JOURNAL OF ELECTRON SPECTROSCOPY and Related Phenomena
www.elsevier.com/locate/elspec

LEEIXS and XPS studies of reactive unbalanced magnetron sputtered chromium oxynitride thin films with air

Saïd Agouram*, Franz Bodart, Guy Terwagne

Laboratoire d'Analyses par Réactions Nucléaires (LARN), Facultés Universitaires Notre-Dame de la Paix, 61, rue de Bruxelles, 5000 Namur, Belgium

Received 5 June 2003; received in revised form 15 October 2003; accepted 17 October 2003

Abstract

Chromium oxynitride thin films were deposited onto polished carbon substrates by an unbalanced magnetron sputtering in a reactive atmosphere of argon and air with different relative humidities (concentrations of water vapor). The composition and thickness of chromium oxynitride thin films were measured by ion beam techniques such as: Rutherford backscattering spectroscopy (RBS) and resonant nuclear reaction analysis (RNRA). The nitrogen and hydrogen profiles were determined by RNRA and Tof-SIMS, the chemical bond analysis was carried out by low energy electron induced X-ray spectroscopy (LEEIXS) and X-ray photoemission spectroscopy (XPS). The LEEIX spectroscopic studies analysis have shown that, during metallic sputtering mode, the composition of Cr–N–O can be fitted only by Cr_2O_3 with low content of CrN and CrO_2, and in the compound sputtering mode the CrO_2 stoichiometry predominates in the presence of low content of CrN. XPS results have also indicated the existence of another compound with $(CrO_2)_3$–N stoichiometry.

Keywords: Chromium oxynitride; LEEIXS; XPS

1. Introduction

Chromium nitride and chromium oxide are very good candidates for protection of steels and decorative applications due to their distinct colors. Like titanium nitride, chromium nitride has good mechanical properties [1,2] and improves corrosion resistance [1,3] because it has high oxidation resistance and a good chemical stability. Like CrN, chromium oxide thin films also present interesting properties such as: a higher hardness [1,4] and beautiful colors intended for decoration [1,5]. Furthermore, other chromium compounds like chromium oxynitride possess promising industrial applications. Chromium oxynitride thin films present various colors, which vary with thickness and composition. In comparison with Cr_2O_3, the chromium oxynitride has a higher corrosion resistance and the layer has a better adhesion and a uniform structure [6]. Collard et al. [1] have synthesized Cr–N–O thin films by reactive sputtering in an atmosphere containing two gases, nitrogen and oxygen. Gautier et al. [7] have applied electric arc method for the deposition of Cr–N–O. The chromium oxynitride films prepared by these two methods (sputtering and

* Corresponding author. Tel.: +32-82-72-44-79; fax: +32-82-72-54-74.
E-mail address: said.agouram@fundp.ac.be (S. Agouram).

0368-2048/$ – see front matter © 2003 Elsevier B.V. All rights reserved.
doi:10.1016/j.elspec.2003.10.004

electric arc) contain two different phases: CrN and Cr_2O_3. Suzuki et al. [8] have produced Cr–N–O thin films using another deposition technique based on a laser beam pulsed in nitrogen and residual oxygen atmosphere. According to the works reported on the Cr–N–O films, it is interesting to produce chromium oxynitride thin films using a reactive plasma with air containing various concentrations of water vapor.

The aim of the present work is to study the influence of relative humidity of air on deposition rate, composition of chromium oxynitride thin films deposited on carbon and to characterize the different phases present in it by means of electronic spectroscopic techniques such as low energy electron induced X-ray spectroscopy (LEEIXS) and X-ray photoemission spectroscopy (XPS).

2. Deposition conditions

The chromium oxynitride films were produced by dc reactive sputtering using an unbalanced magnetron system in an Ar and air gases mixture. The vacuum chamber (0.25 m^3) is equipped with a chromium (99.99% purity) sputtering target disc of 19.6 cm^2 area and a 400 L/min turbomolecular pump. The pressure in the chamber before starting the sputtering process was less than 5×10^{-5} Pa. The deposition working pressure and plasma power density were maintained respectively at 0.56 Pa and 5.86 W/cm^2. Under these conditions, the temperature measured by a thermocouple fixed at the rear end of the substrate during the sputtering process was always less than 100 °C. First, the carbon substrate was polished down to a surface roughness of less than 10 nm and cleaned with distilled water and acetone. Before deposition, pure argon plasma was used to clean the chromium target in order to eliminate the oxide layer formed on the surface of the target. After this the glassy carbon substrate was etched for 4 min in a pure argon plasma atmosphere. High-purity argon and dry air were used and both gas flows were controlled. The reactive gas (air) and argon were admitted separately through a MKS flow control system, keeping a constant total gas flow of 35 sccm for all deposition runs. The reactive gas flow varied from 0% (0 sccm) to 70% (25 sccm). In this work different reactive gases such as dry air, air at 20, 40, 65 and 95% relative humidity (RH) were used.

3. Analysis techniques

The thickness and composition of chromium oxynitride thin films were measured by Rutherford backscattering spectroscopy (RBS) and resonant nuclear reaction techniques at LARN using 2 MV Tandetron accelerator. The RBS technique was performed with 2 MeV α-particles and the scattered particles were detected in a passivated implanted planar silicon (PIPS) surface barrier detector, located at an angle of 175° to the incident beam. The experimental spectra are fitted with the RUMP code [9,10]. The nitrogen and hydrogen profiles were measured by using the narrow resonance nuclear reaction and Tof-SIMS. The ^{15}N (p, α) ^{12}C reaction at $E_p = 429$ keV for nitrogen and H (^{15}N, αγ) ^{12}C reaction at 6.385 MeV for hydrogen profiling were used. The 4.43 MeV γ-radiation of $^{12}C^*$ was measured with a NaI detector as a function of the incident particles energy to obtain the concentration profile. The chemical bond and the composition of the films formed were studied by low energy electron induced X-ray spectroscopy and X-ray photoemission spectroscopy. The LEEIXS is based on the ionization of the inner-shell of the analyzed element by electrons of a few keV. In this work we investigate the intensity measurement of the Cr Lα with a TAP crystal. The energy of the incident electron beam is 5 keV, the gas pressure is 0.23 Torr and the current is 0.12 mA. The measuring parameters of Cr L-spectra are given in Table 1. With 5 keV of electron beam, the thickness of samples analyzed was between 120 and 240 nm. XPS measurements were recorded with a SSX-100 spectrometer using the monochromatised X-ray Al Kα (1486.4 eV) at LISE (Laboratoire Interdépartemental de Spectroscopie Electronique) at FUNPD.

Table 1
Measuring parameters of Cr L-spectra

Crystal	TAP 2d = 25.75
Discharge conditions	Voltage: 5 kV, current: 0.12 mA, pressure: 0.23 Torr
Angle 2θ	106–120°
Step	0.15°

4. Results and discussion

The Cr L experimental spectra were fitted by a linear combination of data obtained from the standard samples (Cr, CrN and Cr_2O_3). In Fig. 1 we present the experimental spectra obtained from standard samples. These X-ray spectra were obtained under condition listed in Table 1.

In the pure chromium spectrum we observed two peaks which correspond to the two main transitions, Lα and Lβ. In the case of the L X-ray spectra of chromium obtained from chromium nitride

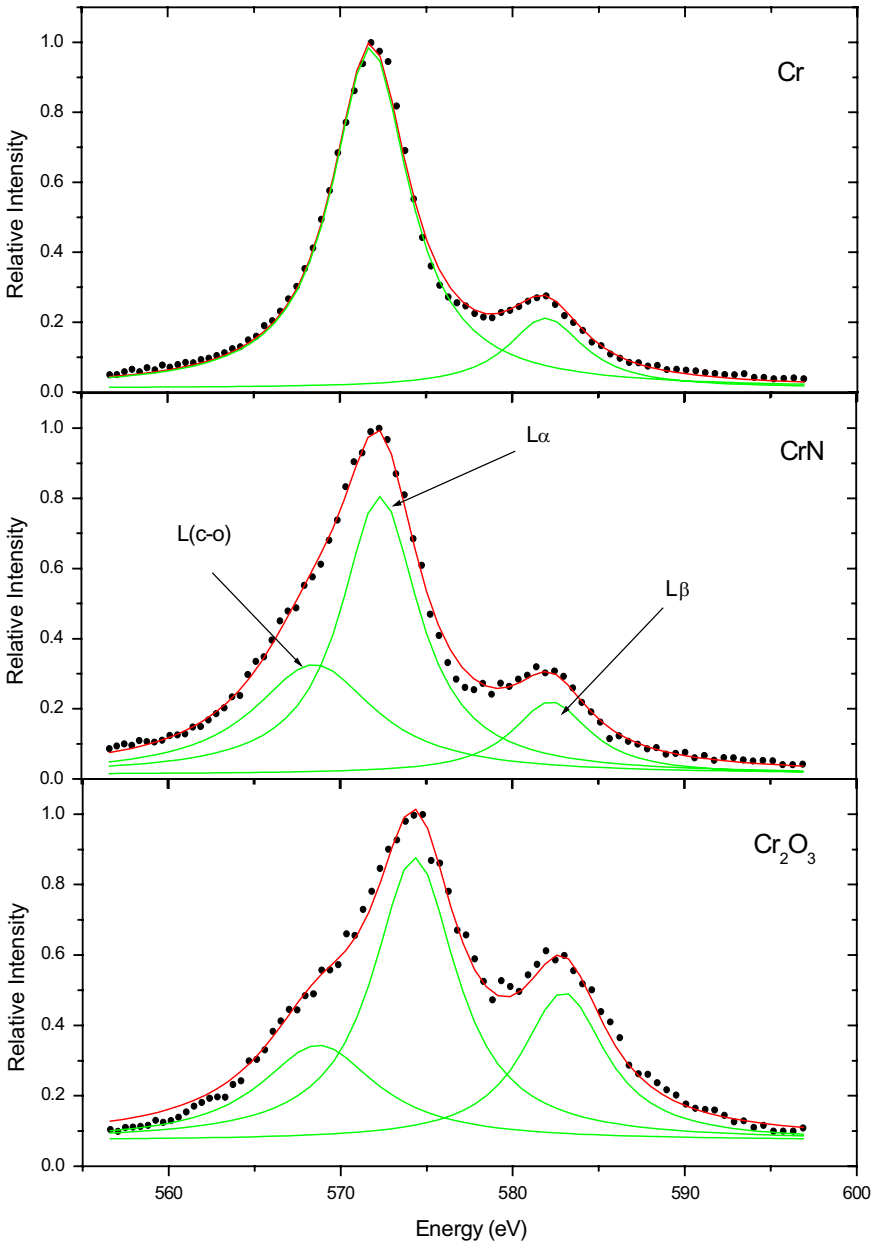

Fig. 1. Normalized Cr L-spectra obtained from the standard samples (Cr, CrN and Cr_2O_3).

Table 2
Spectra data of Cr L-transitions

	Cr	CrN	Cr_2O_3
Max Lβ (eV)	581.9 ± 0.2	582.3 ± 0.2	582.96 ± 0.2
Half width	5.5 ± 0.5	5.5 ± 0.4	5.9 ± 0.4
Max Lα (eV)	571.8 ± 0.1	572.3 ± 0.1	574.3 ± 0.1
Half width	5.5 ± 0.3	5.6 ± 0.3	5.9 ± 0.3
Max crossover (eV)		568.3 ± 0.5	568.7 ± 0.2
Half width		8.54 ± 0.4	8.2 ± 0.5
Intensity ratio: max Lα/ max Lβ	4.76 ± 0.5	3.77 ± 0.7	1.92 ± 0.2
max Lα/max Lco		1.5 ± 0.6	2.13 ± 0.2

and chromium oxide, we observed three peaks Lβ Lα, and Lco. The first peak (Lβ) is attributed to a Cr(3d) → Cr(LIII) transition, the second peak (Lα) is attributed to a Cr(MIV) → Cr(LIII) transition. The peak (Lco) at low energy is a "crossover transition" 2p (O, N) → Cr(LIII). The fundamentals of soft X-ray Spectroscopy can be found in the literature [11–16]. The experimental data obtained from standard sample are given in Table 2.

The deconvolution of experimental spectra obtained from chromium oxynitride samples works on the basis of the "non-linear least squares" method; it is obtained by repeatedly modifying the peak area with respect to the parameters given in Table 2 (FWHM, intensity ratio and energy difference between peaks Lα, Lβ and crossover) obtained from standard sample. Fig. 2 presents an example of Cr L X-ray spectra obtained under the same conditions listed in Table 1, from chromium oxynitride sample deposited under 5 and 15 sccm of dry air flow. The decomposition of the Cr L X-ray spectra taken from chromium oxynitride samples allowed identifying the compounds existing in Cr–N–O thin films. In case of chromium oxynitride thin film produced with 5 sccm of reactive gas we observe the contribution of the three peaks characteristic of chromium nitride (CrN) and chromium oxide (Cr_2O_3). In case of sample produced with 15 sccm of air flow, we observe the three peaks characteristic of CrN and other three peaks can be attributed to CrO_2 (it is interesting to note that we do note have a CrO_2 standard sample). The experimental position peaks is: the first peak is Lβ at 582 ± 0.2 eV, the second Lα at 573.9 ± 0.2 eV and the third corresponds to crossover transition at 568.2±0.2 eV. With this method we could determine the proportions of each compound and follow the variations with gas flow and relative humidity. The results of this analysis are shown in Fig. 3.

We observe, during sputtering in metallic mode, that the Cr_2O_3 stoichiometry is in majority with a small percentage of CrN and CrO_2. This can be explained by the fact that enthalpy of formation of Cr–N at 25 °C is −29.8 kcal/(g mol), very low value (absolute value) in comparison with that of chromium oxide Cr_2O_3 −269.7 kcal/(g mol) [17]. When air flow and relative humidity are increased, the content of CrO_2 increases while the Cr_2O_3 concentration decreases. During sputtering in compound mode, we observe the existence of

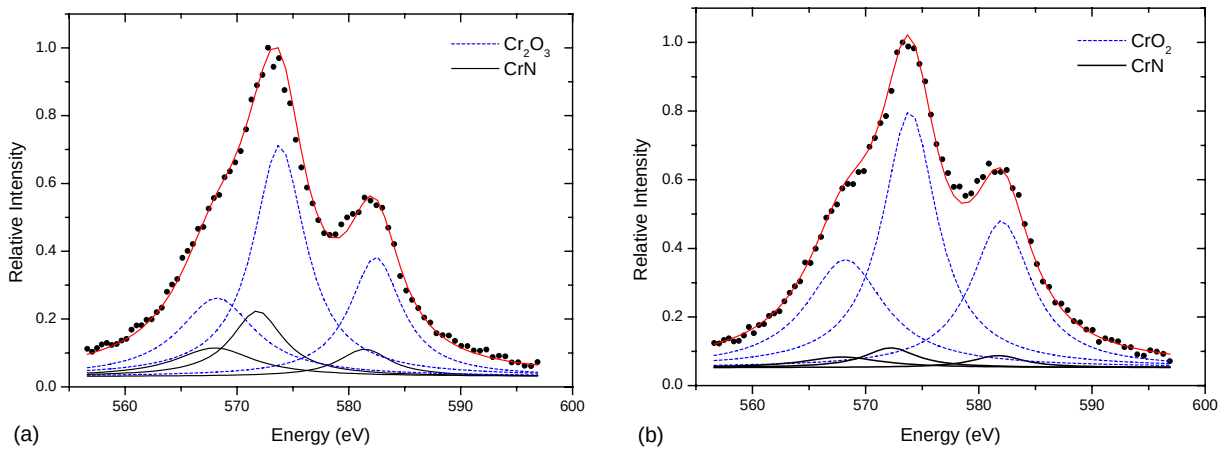

Fig. 2. Cr L-spectra obtained from oxynitride sample deposited on carbon substrate at 5 and 15 sccm air flow.

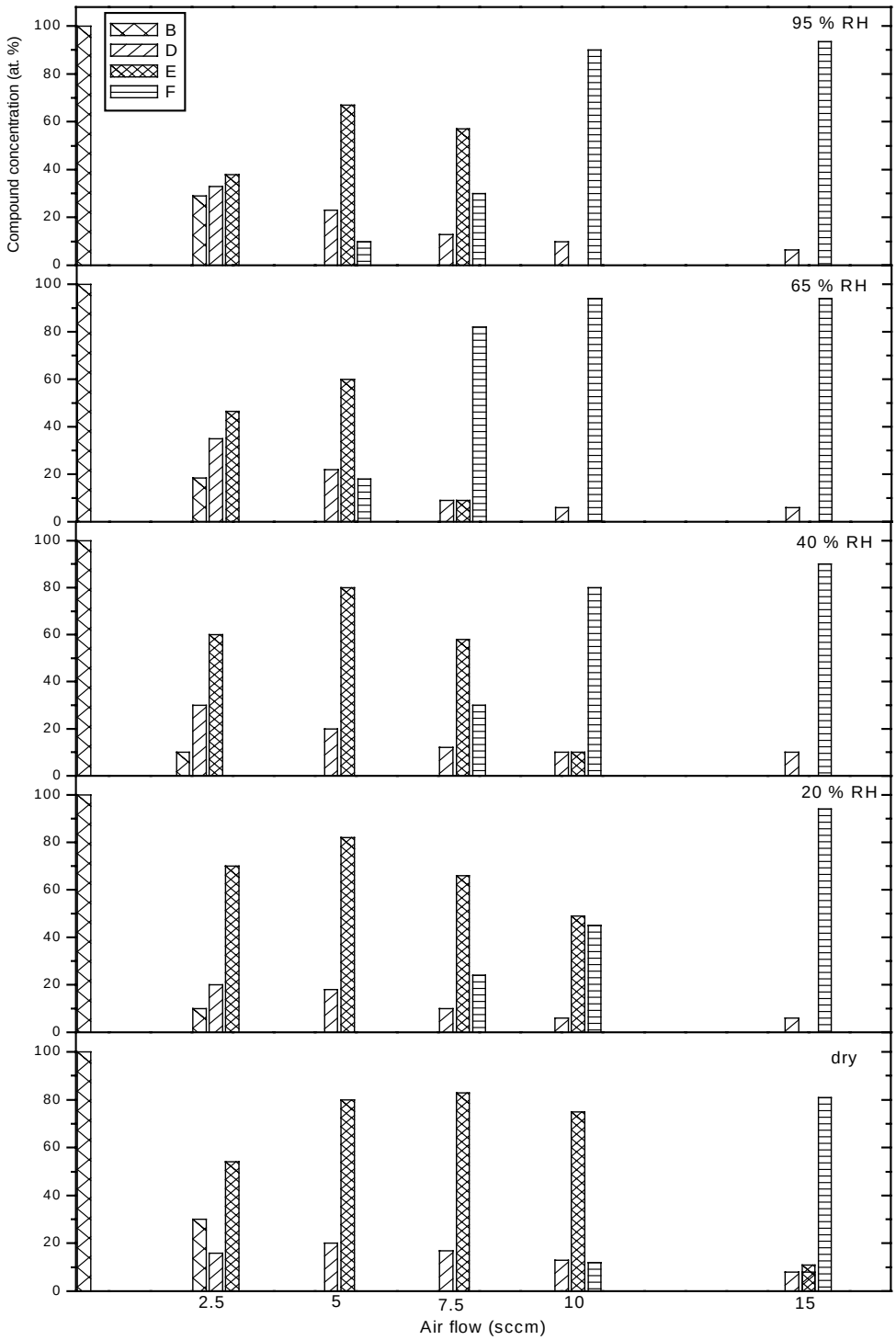

Fig. 3. Evolution of Cr and compound content determined by LEEIX spectroscopy as a air flow and relative humidity.

Table 3
Cr, O, N and H concentrations in chromium oxynitride thin films determined by different techniques (RBS, LEEIXS, XPS and RNRA)

Sample	Element	Atomic concentration ± 2.5 at.% (RBS)	Atomic concentration ± 10 at.% (LEEIXS)	Atomic concentration at.% (XPS)	Atomic concentration at.% RNRA	Thickness (nm)
Cr–N–O/C 5 sccm dry air	Cr	42	46	38.5		240
	O	46	44	55.5		
	N	12	10	6	14.0	
	H				1.0	
Cr–N–O/C 10 sccm dry air	Cr	39	40.5	38.9		240
	O	55	53	59.3		
	N	6	6.5	1.8	4.0	
	H				2.0	
Cr–N–O/C 5 sccm air at 65% RH	Cr	40	41	36		240
	O	48	47	61		
	N	12	12	3	17.5	
	H				3.0	
Cr–N–O/C 10 sccm air at 65% RH	Cr	34	34.3	36.8		120
	O	64	62.7	61.7		
	N	2	3	1.5	3.0	
	H				11.0	
Cr–N–O/C 5 sccm air at 95% RH	Cr	38.5	42.3	36.9		240
	O	48	46.2	59.5		
	N	13.5	11.5	3.6	15.5	
	H				6.0	
Cr–N–O/C 10 sccm air at 95% RH	Cr	33.5	35	36.9		120
	O	62	60	61.9		
	N	4.5	5	1.2	3.0	
	H				11.0	

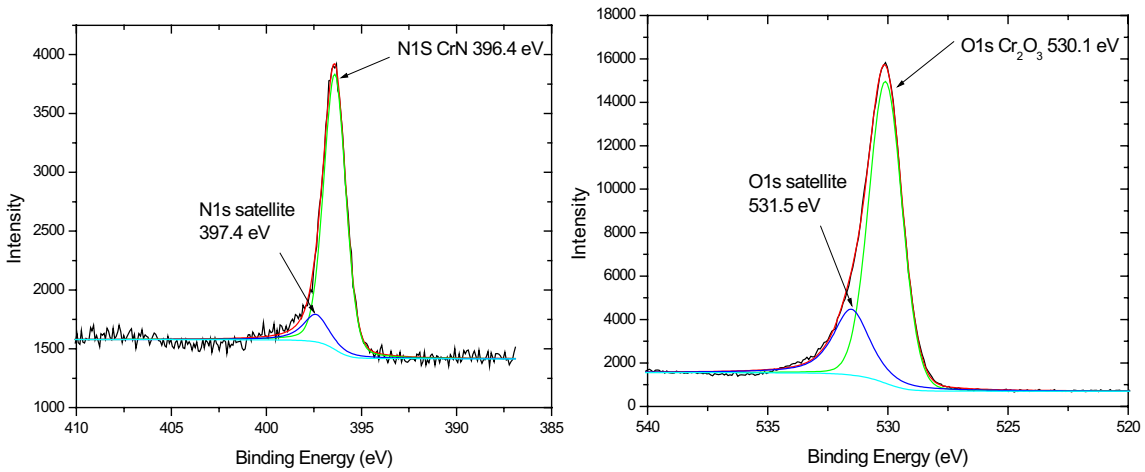

Fig. 4. N 1s and O 1s XPS spectra for chromium oxynitride sample deposited with 5 sccm dry air flow.

two different compounds CrO_2 and CrN. In this mode of sputtering, relative humidity does not affect the proportions of the compounds formed and CrO_2 (90%) stoichiometric predominates in coexistence with low contents of CrN (10%). The Cr, O, N and H contents obtained by various techniques are given in Table 3.

The LEEIXS results are completed by XPS measurements of Cr 2p, O 1s and N 1s. In order to eliminate the carbon and oxygen contamination on the surface, all samples were sputtered with Ar^+ ions for 1 min with energy equal to 2 keV and an emission current with intensity equal to 10 mA. In Fig. 4, we present two XPS spectra (N 1s and O 1s) from chromium oxynitride film deposited with 5 sccm of dry air flow. Fig. 5 gives O 1s XPS spectra of the samples deposited with 5 and 10 sccm of air at 65% RH.

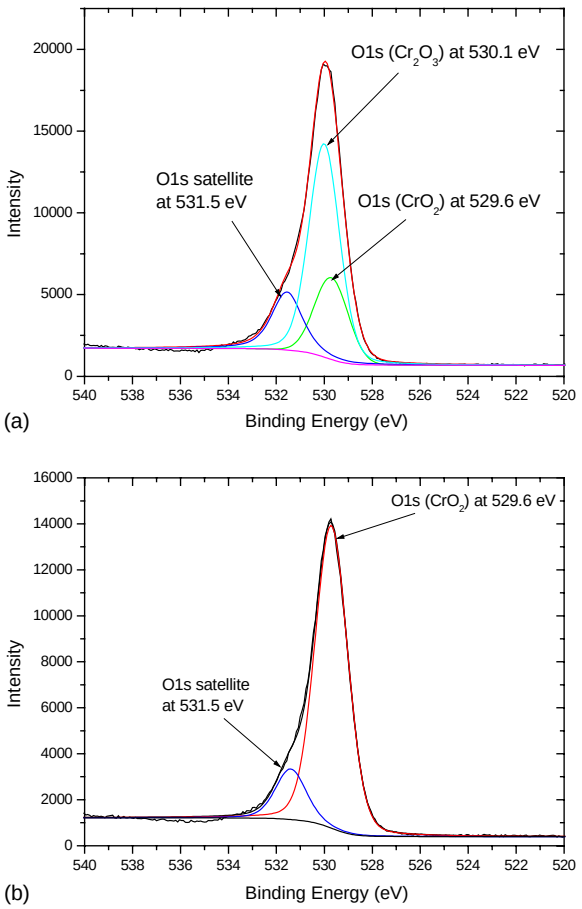

Fig. 5. O 1s XPS spectra for chromium oxynitride sample deposited with 5 sccm (a) and 10 sccm (b) of air at 65% RH.

In Fig. 4, the decomposition of the N 1s peak clearly shows the existence of two components: a major component at 396.4 ± 0.1 eV attributed to N 1s from CrN in agreement with the literature value 396.6 ± 0.2 eV [18] and a second component, called satellite peak, at 397.4 ± 0.1 eV. Furthermore, the decomposition of O 1s peak reveals the presence of two peaks, the first one at 530.1 ± 0.1 eV, which corresponds to the O 1s from Cr_2O_3 also in agreement with the literature value of 530.2 ± 0.2 eV [18] and the second peak (satellite) at 531.5 ± 0.1 eV.

In Fig. 5a, simulation of O 1s XPS spectra clearly shows the existence of three O 1s components. A first component at 529.6 ± 0.1 eV, which can be attributed to the O 1s coming from CrO_2 in agreement with the literature value of 529.3 eV [19]. The second component at 530.1 ± 0.1 eV corresponds to the O 1s from Cr_2O_3, and a third satellite component at 531.5 ± 0.1 eV. In the case of the XPS spectrum (Fig. 5b) sample with 10 sccm of air 65% RH (b), we observe the presence of two peaks, at 529.6 ± 0.1 eV characteristic of CrO_2 and a satellite peak at 531.5 ± 0.1 eV. The presence of the two satellite lines N 1s (397.4 eV) and O 1s (531.5 eV) could be attributed to a different chromium compound containing nitrogen and oxygen like $Cr_xN_yO_z$ type.

The N 1s and O 1s satellite peak areas are used to determine the stoichiometry of $Cr_xN_yO_z$ compound and was found to be $(CrO_2)_3$–N. It is obvious from three CrO_2 grouping with a nitrogen incorporation which disturbs the O–Cr bond to give a satellite peak O 1s at 531.5 eV and another satellite peak N 1s at 397.4 eV. However it is not known if this nitrogen is close or free in the CrO_2 networks. The percentage of $(CrO_2)_3$–N present in each of the samples could be deduced from the percentages of the satellite peaks O 1s and N 1s and the content of $(CrO_2)_3$–N varies according to the air flow and relative humidity (Fig. 6).

From the variations of the concentration in $(CrO_2)_3$–N (Fig. 6), we note that with 5 sccm air flow, the content of $(CrO_2)_3$–N increases to the detriment of Cr_2O_3 concentration according to relative humidity and reaches a maximum when the relative humidity is 65% RH. At 10 sccm of air flow, the content of $(CrO_2)_3$–N decreases according to the relative humidity whereas the content of CrO_2 increases. The variations of the content of $(CrO_2)_3$–N can be related to the amount of CrO_2 and nitrogen in chromium oxynitride thin films. At 5 sccm of air flow, the thin

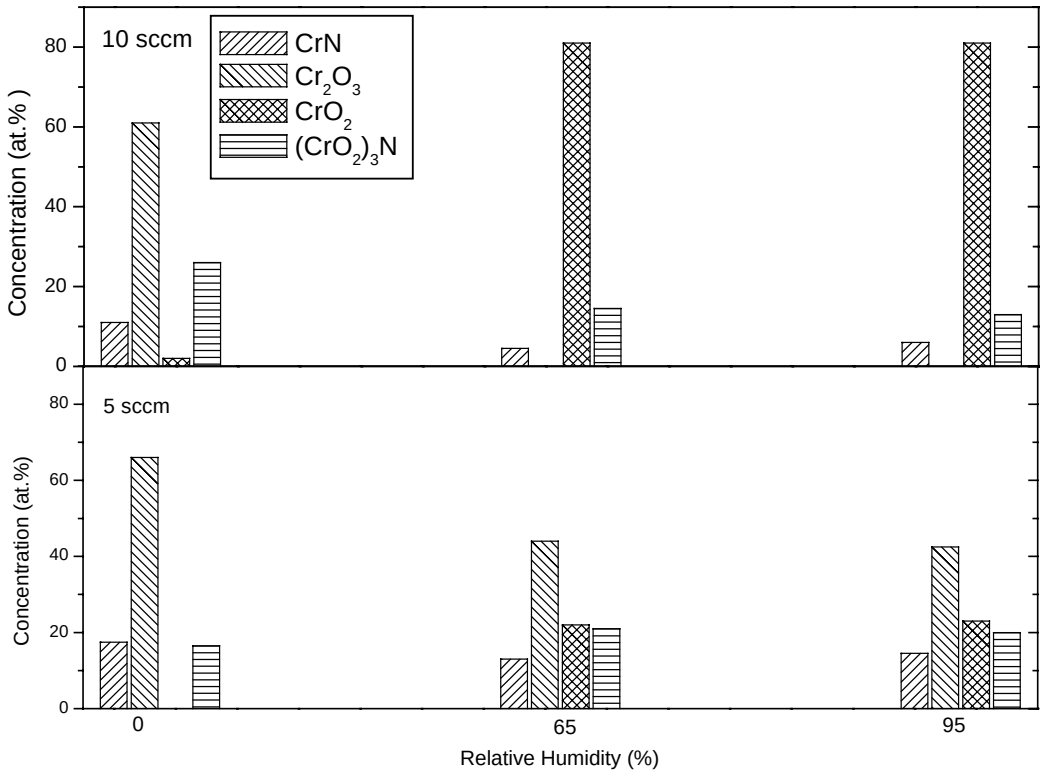

Fig. 6. Evolution of Cr and compound content determined by LEEIX spectroscopy and XPS as a air flow and relative humidity.

films, which contain CrO_2 and nitrogen (>3%) exhibit a significant content of $(CrO_2)_3$–N. On the other hand, films containing a low nitrogen content (±1%) show a small proportion of $(CrO_2)_3$–N.

In conclusion, relative humidity accelerates the formation of CrO_2 and $(CrO_2)_3$–N to the detriment of Cr_2O_3 while the content of $(CrO_2)_3$–N is proportional to the nitrogen content in chromium oxynitride thin films.

5. Conclusion

The LEEIXS and XPS measurements provide useful information about the nature of the formed compounds. Indeed, XPS results revealed the presence of a compound other than CrN, Cr_2O_3 and CrO_2, determined by the LEEIXS. This compound contains nitrogen and oxygen and it has a $(CrO_2)_3$–N stoichiometry. Currently it is not known if this nitrogen is close to or free in CrO_2 network. In a metallic sputtering mode, when the films contain a significant amount of nitrogen (higher than 3 at.%), relative humidity favors the formation of $(CrO_2)_3$–N to the detriment of Cr_2O_3 phase whereas the quantity of CrO_2 is close to that of $(CrO_2)_3$–N. When the compound sputtering mode is installed, the nitrogen quantity is very weak, and does not exceed 1.5 at.% The content of $(CrO_2)_3$–N decreases whereas that of CrO_2 increases with an increase in relative humidity and it stabilized to 81% when the relative humidity reaches 65%. In this deposition mode the Cr_2O_3 compound is not observed. Tof-SIMS profiles showed that the chromium oxynitride thin films do not present an inhomogeneity in the profile of concentration.

References

[1] St. Collard, H. Kupfer, G. Hecht, W. Hoyer, H. Moussaoui, Surf. Coat. Technol. 112 (1999) 181–184.
[2] W. Herr, Surf. Coat. Technol. 60 (1993) 428.

[3] E. Ertürk, H.J. Heuvel, in: R.-J. Peter (Ed.), Beschichten mit Harstoffen, VDI, Düsseldorf, 1991, p. 250.
[4] R. Elsing, in: R.-J. Peter (Ed.), Beschichten mit Harstoffen, VDI, Düsseldorf, 1991, p. 1.
[5] JCPDS-Data files, no. 38–1479, International Center For Diffraction Data, Swarthmore, 1992.
[6] T. Wierzchon, I. Ulbin-Pokorska, K. Sikorski, Surf. Coat. Technol. 130 (2000) 274–279.
[7] C. Gautier, J. Machet, Surf. Coat. Technol. 94–95 (1997) 422–427.
[8] T. Suzuki, H. Saito, M. Hirai, H. Suematsu, W. Jiang, K. Yatsui, Thin Solid Films 407 (1–2) (2002) 118–121.
[9] L. Doolittle, Algorithms for the rapid simulation of Rutherford backscattering spectra, Nucl. Instrum. Methods B9 (1985) 344.
[10] L. Doolittle, A semi-automatic algorithms for the rapid simulation of Rutherford backscattering analysis, Nucl. Instrum. Methods B15 (1986) 227.
[11] C.J. Powell, Reviews of Modern Physics, vol. 48 (1), January 1976.
[12] E. Pappert, J. Flock, J.A.C. Broekert, Spectrochim. Acta Part B 54 (1999) 299–310.
[13] M. Romand, F. Gaillard, M. Charbonnier, Plasma Surface Engineering, vol. 2, DGM Information Gesellshaft Verlag, Oberursel, 1989, pp. 759–766.
[14] M. Romand, F. Gaillard, M. Charbonnier, Adv. X-ray Anal. 35 (1992) 767–781.
[15] M. Romand, M. Charbonnier, J. Baborowski, Journal de Physique IV 6 (Juillet 1996) C4-467–C4-474.
[16] M. Romand, R. Bador, M. Charbonnier, F. Gaillard, X-ray Spectrom. 16 (1987) 7–16.
[17] R. Weast, Handbook of Chemistry and Physics, CRC Press, 1975.
[18] XPS Standard Data Base, http://www.srdata.nist.gov/xps/.
[19] I. Ikemoto, Solid State Chem. 17 (1976) 425.